Journal of Applied Polymer Science

Composite chitosan/poly(ethylene oxide) electrospun nanofibrous mats as novel wound dressing matrixes for the controlled release of drugs

Feng Cheng, Jing Gao, Lu Wang, Xingyou Hu
Key Laboratory of Textile Science and Technology (Ministry of Education), College of Textiles, Donghua University, Shanghai 201620, China
Correspondence to: J. Gao (E-mail: gao2001jing@dhu.edu.cn)

ABSTRACT: The aim of this study was to develop novel biomedical electrospun nanofiber mats for controlled drug release, in particular to release a drug directly to an injury site to accelerate wound healing. Here, nanofibers of chitosan (CS), poly(ethylene oxide) (PEO), and a 90:10 composite blend, loaded with a fluoroquinolone antibiotic, such as ciprofloxacin hydrochloride (CipHCl) or moxifloxacin hydrochloride (Moxi), were successfully prepared by an electrospinning technique. The morphology of the electrospun nanofibers was investigated by scanning electron microscopy. The functional groups of the electrospun nanofibers before and after crosslinking were characterized by Fourier transform infrared spectroscopy. X-ray diffraction results indicated an amorphous distribution of the drug inside the nanofiber blend. *In vitro* drug-release evaluations showed that the crosslinking could control the rate and period of drug release in wound-healing applications. The inhibition of bacterial growth for both *Escherichia coli* and *Staphylococcus aureus* were achieved on the CipHCl- and Moxi-loaded nanofibers. In addition, both types of CS/PEO and drug-containing CS/PEO nanofibers showed excellent cytocompatibility in the cytotoxicity assays. © 2015 Wiley Periodicals, Inc. J. Appl. Polym. Sci. **2015**, *132*, 42060.

KEYWORDS: biomaterials; biomedical applications; electrospinning; fibers

Received 28 October 2014; accepted 25 January 2015
DOI: 10.1002/app.42060

INTRODUCTION

Electrospinning is currently one of the most inexpensive, effective, and versatile methods for producing nonwoven nanofibrous mats, which generate various synthetic and natural polymer fibers with small diameters, ranging from 10s of nanometers to a few micrometers.[1–5] Several natural polymers and a variety of synthetic polymers, such as cellulose and its derivatives, chitosan (CS),[6,7] collagen,[8,9] sodium alginate,[10,11] silk fibroin,[12] gelatin,[13] poly(lactic-*co*-glycolide),[14] poly(ε-caprolactone),[15] and polyurethane,[16] have been successfully electrospun into nanofibers. Nanofiber mats have been shown to have several characteristic properties, including a small fiber size, extremely large specific surface, high porosity, and low fabric weight, that are conducive to drug release, absorbency, and the proliferation of wound healing.[1–3,17] The three-dimensional porous networks of electrospun nanofibers generate structures similar to natural extracellular matrix elements,[18,19] which are interesting for use in wound-healing processes.

CS, as one of the most abundant natural polysaccharides, is very similar to cellulose except for the amino group replaced the hydroxyl group on the C-2 site.[20,21] CS is well known for its extraordinary biological characteristics; it is nontoxic, nonantigenic, biodegradable, biocompatible, antibacterial, and hemostatic.[22–24] However, its unique polycationic nature in solution, rigid chemical structure, and interaction of intermolecular and intramolecular hydrogen bonding restrict sufficient chain entanglements for fiber formation;[25,26] thus, the electrospinning of pure CS is still limited.

To date, several research groups have created composite CS nanofibers with other synthetic biodegradable polymers in an attempt to improve the electrospinnability of CS; these include poly(ethylene oxide) (PEO)[4,6,27,28] and poly(vinyl alcohol).[29–32] In the blends, the fiber-forming ability is improved through the adjustment of the interaction between polymer molecules without the creation of phase separation.[27] Because of its good biocompatibility and low toxicity, PEO has attracted increasing interest for its applications in biomedical fields. As a polymer well-suited for fiber formation in many solvents, especially water, its feasibility and versatility for electrospinning have been widely documented.[33]

In recent years, a few reports have considered the introduction of organic antibacterial agents into natural antibacterial materials to enhance the antimicrobial properties of nanofibers used in wound healing. For example, Dilamian *et al.*[6] prepared CS/PEO nanofibrous incorporating poly(hexamethylene biguanide) hydrochloride. Jannesari *et al.*[34] prepared poly(vinyl alcohol)/poly(vinyl acetate) electrospun nanofibrous mats loaded with

ciprofloxacin hydrochloride (CipHCl). Unnithan *et al.*[19] prepared electrospun polyurethane–dextran nanofiber mats containing CipHCl. CipHCl and moxifloxacin hydrochloride (Moxi) are the most widely used fluoroquinolone antibiotics in wound healing because of their low frequency of spontaneous resistance[35,36] and low minimal inhibitory concentration for both Gram-positive and Gram-negative bacteria.[37,38]

Chemical crosslinking by glutaraldehyde (GA) vapor of the nanofibers is often performed to maintain the structural integrity *in vivo*, control the release rate of the active ingredients from the nanofiber mats, and improve the tensile strength of the nanofibers.[24,30]

In this study, the main objective was to improve the antibacterial properties of the composite CS/PEO nanofibers through the incorporation of CipHCl and Moxi for wound-dressing applications. CS/PEO nanofibrous mats loaded with CipHCl and Moxi, respectively, were formed by electrospinning. The nanofiber size and morphology were characterized, and the tensile strength, antibacterial properties, and CipHCl and Moxi release properties of the nanofiber mats were investigated.

EXPERIMENTAL

Materials

CS (95.28% deacetylated, the viscosity of a 1% solution in 1% v/v acetic acid was 235 MPa s) was obtained from Zhejiang Golden-Shell Biological Co., Ltd. (China). Poly(ethylene oxide) (PEO; weight-average molecular weight = 900 kDa) was obtained from J&K Chemical Co. Acetic acid (99.9%), a GA aqueous solution (25%), and glycine were purchased from Sinopharm Chemical Reagent Co., Ltd. (China). The fluoroquinolone antibiotics, CipHCl and Moxi, were purchased from Xi'an Bochang Biological Technology Co., Ltd. (China). All of the reagents were used without further purification.

Preparation of the Drug–CS/PEO Electrospinning Solution

CS and PEO powders were mixed at a weight ratio of 90/10 and then dissolved in 90 wt % aqueous acetic acid at a polymer concentration of 3–5 wt %. The mixtures were stirred at room temperature for 12–24 h with a magnetic stirrer (Corning, Inc., MA) to ensure complete dissolution of the polymers and to obtain homogeneous solutions. The prepared solutions were left to rest for 1 h for degassing and kept in sealed containers at room temperature. CipHCl or Moxi powder (5 or 10 wt % of the polymer used) was added to the polymer solutions. All of the solutions were then used immediately for electrospinning.

Preparation of the Pure and Drug-Loaded Nanofiber Mats

The electrospinning solution was transferred to a 5-mL syringe pump with a needle (gauge 20) attached to it. The resulting fibers were collected on a grounded aluminum plate. All of the electrospinning processes were carried out at 15–25 °C. The solution flow rate was 0.5–1.0 mL/h, a positive voltage range of 8–25 kV was applied to the collecting target by a high-voltage power supply, and the distance between the needle tip and the target was 20 cm. The mats thickness was measured with a thickness tester (CH-12.7-BTSX, China). The thickness of the electrospun nanofiber mats ranged from 30 to 60 μm.

Crosslinking

Nanofiber mats with dimensions of 6 × 6 cm^2 were placed on an empty vapor container at room temperature in a ventilated hood. The nanofibers were not removed from the release cloth. Twenty-five milliliters of room-temperature 25% w/v GA aqueous solution was pipetted into the container and evenly dispersed. GA crosslinked with the nanofibers through vapor deposition as the GA vaporized to the top of the container, where the samples were located. Nanofiber mats were crosslinked for 8 h. Unreacted GA in the nanofiber mat was quenched by overnight immersion in a 0.2*M* glycine solution. The nanofiber mats were then washed repeatedly in phosphate-buffered saline (PBS). The crosslinked nanofiber mats were dried and stored in plastic bags in a desiccator.

Morphology of the Electrospun Nanofibers

The surface morphologies of the electrospun nanofibers were investigated with scanning electron microscopy (SEM; Hitachi, TM-3000, Japan). The samples were sputter-coated with gold for better conductivity during imaging. To determine the average fiber diameters and their distributions for each electrospun mat, from each image, at least 100 different fiber segments were randomly selected, and the diameters were measured in Adobe Acrobat 9 Pro software.

Fourier Transform Infrared (FTIR) Spectroscopy

The local compositional and chemical characteristics of the samples were evaluated by FTIR spectroscopy measurements on a Nicolet 5700 instrument (Thermo Co.). The samples were prepared as nanofiber mats and were scanned against an air background at wave numbers ranging from 4000 to 500 cm^{-1} with a 4.0-cm^{-1} resolution. Measurements were performed on CS powder, as-spun PEO, CS/PEO, CipHCl and Moxi powder, and CS/PEO/CipHCl and CS/PEO/Moxi blend nanofibrous mats.

X-ray Diffraction (XRD) Studies

XRD was used to investigate the effect of electrospinning on the degree of crystallization of the drug and the influence of the drug on the crystalline structure of the polymer nanofibers. The samples were recorded over a diffraction angle (2θ) that ranged from 5 to 40°. The XRD patterns of the pure CipHCl and Moxi and blend nanofiber mats with and without drugs were determined with a diffractometer (Rigaku D/max-2550 PC, Japan).

In Vitro Drug Release of the Medicated Nanofiber Mat Studies

The release characteristic of CipHCl and Moxi from electrospun nanofiber mats was measured by the immersion of a known mass of material (30 mg) in 8 mL of PBS (pH 7.2–7.4) in centrifuge tubes, which were kept in a shaking incubator with a shaking speed of 60 rpm at 37 °C. At procedural time points, a 1.0-mL solution was taken out, and an equal amount of the fresh buffer solution was supplemented. The absorption intensity of CipHCl and Moxi was determined by an ultraviolet–visible spectrum (TU-1901, China) at the maximal absorption peak with wavelengths of 280 and 283 nm. The release experiments of each specimen were performed in triplicate, and the average values are reported.

Antibacterial Activity Test

The antibacterial activity test against *Staphylococcus aureus* (SA) ATCC 25923 and *Escherichia coli* (EC) ATCC 25922 were carried out using agar disc diffusion method with determination of the inhibition zones (mm). The samples were cut into small circular pieces (10 mm). The control sample was prepared by CS nanofibers without drugs. The plates were filled with sterilized Luria–Bertani agar medium. A transferring loop of bacteria was taken and dispersed on the surface of slope medium evenly, after the plates were inoculated, the samples were placed on them and they were placed in the incubator at 37 °C for 18–24 h. After incubation, the diameters of the growth inhibition zones were measured.

In Vitro Cell Culture

The cytotoxicity of the electrospun nanofiber mats were evaluated on the basis of a procedure adapted from the ISO 10993-5 standard test method. Porcine endothelial cells (PIECs; Department of biology, Donghua University, China) were cultured in Dulbecco's modified Eagle medium (Gibco, United States) supplemented with 10% fetal bovine serum (Gibco USA). The culture was maintained at 37 °C in a wet atmosphere containing 5% CO_2. When the cells reached 80% confluence, they were trypsinized with 0.25% trypsin and 0.02% ethylenediamine tetraacetic acid (Jinuo Biomedical Technology Co., Ltd., China).

AlamarBlue (ALB) Assay

The viabilities of the cells were determined by an ALB assay. For the ALB assay, the nanofiber mats were cut into circular mode 12 mm in diameter. The prepared samples were sterilized with alcohol steam for 24 h and then washed thoroughly with a sterilized PBS solution three times before they were transferred to individual 24-well tissue culture plates. The samples were prewetted by immersion in cell culture medium for 4 h. PIECs cultured in a 25-cm^2 cell culture flask were trypisinized, counted, and plated at a density of 2×10^4 cells/well. Then, 400 μL of fresh culture medium was added to each well and after incubation for 20 h, and then, 40 μL of ALB reagent was added. After 4 h, the medium in 24-well tissue culture plates was transferred to 96-well culture plates, and the optical density value was measured by an enzyme-labeled meter at 570 nm.

RESULTS AND DISCUSSION

Morphological Structure Studies

The morphologies of the electrospun nanofibers are demonstrated in Figure 1. Pure CS did not form fibers, and only beads or drops were deposited.[27,39] To addressed this problem, PEO was added to the CS solution; this could disrupt the self-association of CS chains by the formation of additional hydrogen bonding between its hydroxyl groups and water molecules. This led to a reduction in the repulsive forces between polycationic groups, improved chain entanglement, and induced the production of fibers. The effects of the blend composition and acetic acid concentration on the properties, such as the surface tension, conductivity, and ultrafine fiber structure, were considered.[27,28] As shown in Figure 1(a), no beaded CS/PEO nanofibers were successfully produced. Figure 1(b,c) shows SEM images of the nanofibers; no beaded nanofibers and no drug crystals were detected on the nanofibers loaded with 5–10 wt % CipHCl or Moxi at a CS/PEO ratio of 90/10. The introduction of drugs did not affect the appearance of the nanofiber mats. Both the average diameters of the electrospun structures containing 5 and 10 wt % drugs decreased compared with the nanofibers without drugs. For nanofiber-loaded CipHCl, the diameters decreased from 310 to 238 and 191 nm, respectively. For nanofibers loaded with Moxi, their diameters decreased to 305 and 240 nm, respectively. The possible reason may have been decreases in the conductivity and viscosity of the solution after the addition of drugs, which could have affected the morphological structure and average diameter of the nanofibers.[6,40–42]

FTIR Spectroscopy

As shown in Figure 2, the main characteristic band of the pure CS [Figure 2(b)] due to N—H and —OH stretching vibrations and intermolecular hydrogen bonding of the CS backbone was detected at 3558 cm^{-1}. Feature peaks of amide groups and amino groups (O=CR—NH blending vibration) were observed at 1650 and 1594 cm^{-1}, respectively. The peaks at 2873 and 1419 cm^{-1} were attributed to CH_2 stretching and CH/OH vibrations, and other peaks at 1152, 1067, and 1031 cm^{-1} were due to the vibration of C—O—C. A characteristic absorption peak observed at 2885 cm^{-1} for PEO [Figure 2(a)] was assigned to CH_2 stretching vibrations; other typical bands were observed at 1148, 1101, 1062, and 958 cm^{-1} due to C—O—C stretching. With the addition of PEO, the vibration bands of amino (1594 cm^{-1}), amide (1650 cm^{-1}), and hydroxyl (3358 cm^{-1}) groups of CS shifted to 1558, 1620, and 3362 cm^{-1}, respectively. In addition, the vibration peaks of CH_2 [Figure 2(b)] of PEO changed to a lower frequency. The changes may have been due to the intermolecular hydrogen bonding of CS molecules and the formation of new hydrogen bonds among amino, amide, and hydrogen groups in PEO and CS, respectively. After crosslinking with GA vapor, the primary amine peak intensity decreased, and a new peak for C=N imine appeared. This appeared as a strong split peak at 1652 cm^{-1}, and the peak at 1558 cm^{-1} [Figure 2(c)] disappeared because of the loss of free amines in the GA-crosslinked CS nanofibers through the Schiff base mechanism [Figure 2(d)].[6,43] With the addition of CipHCl or Moxi to the CS/PEO solution, the typical peaks for CS and PEO remained unchanged except for their intensity. The absorption intensity of NH_2 groups at 3353 cm^{-1} (N—H stretching) decreased after the addition of CipHCl increased slightly at 3359 cm^{-1} (N—H stretching) after the addition of Moxi. The intensity of C=N imine groups at about 1625 cm^{-1} increased [Figure 2(g,h)]. Moreover, the amide group peak at 1558 cm^{-1} slightly shifted to 1568 and 1567 cm^{-1} after the additions of CipHCl and Moxi, respectively. The shifts may have been caused by the repulsive forces of cationic CipHCl, Moxi, and CS and the formation of new hydrogen bonds between oxygen and hydrogen from CipHCl, Moxi, and PEO, respectively.

XRD Studies

As shown in Figure 3, XRD was used to further illustrate the structure and drug distribution in the composite nanofibers. A typical broad peak around $2\theta = 20.1°$ corresponded to the CS crystal structure [Figure 3(a)], whereas the peak at 20.6° was

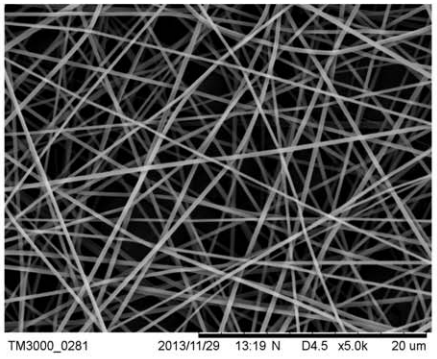

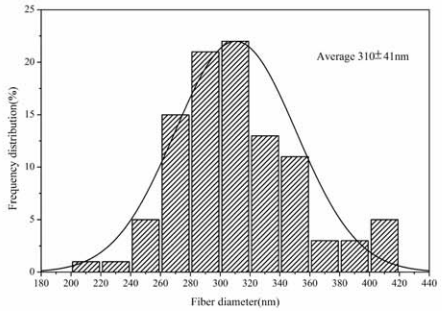

(a)

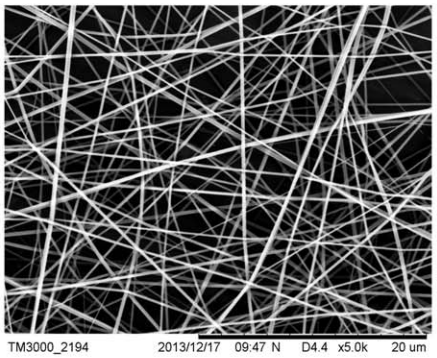

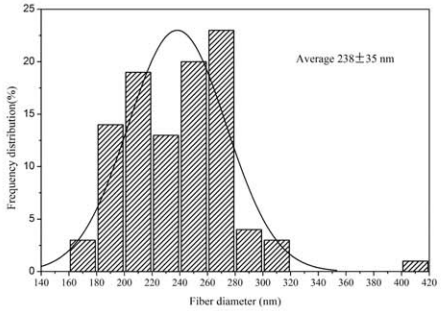

(b)

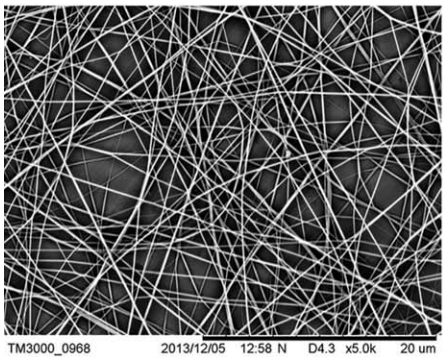

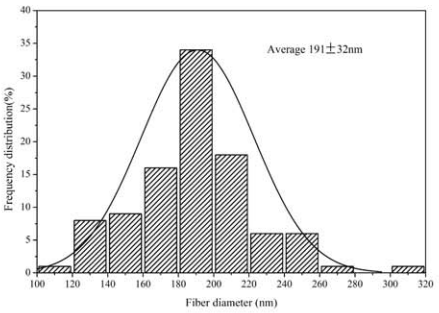

(c)

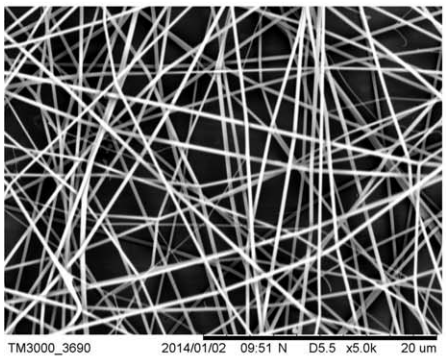

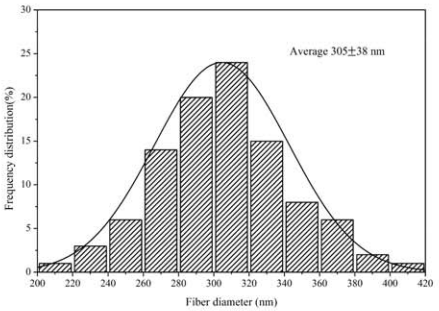

(d)

Figure 1. SEM images and diameter distribution histograms of the (a) electrospun nanofibers without the drug, (b) 5 wt % CipHCl–CS/PEO nanofibers, (c) 10 wt % CipHCl–CS/PEO nanofibers, (d) 5 wt % Moxi–CS/PEO nanofibers, and (e) 10 wt % Moxi–CS/PEO nanofibers.

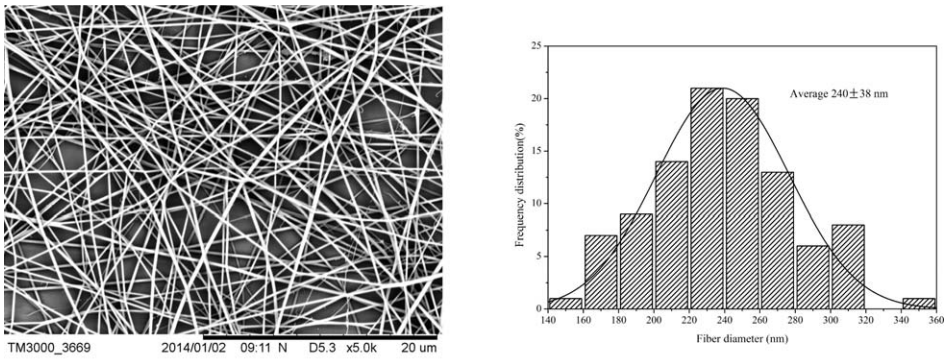

(e)

Figure 1. (Continued)

attributed to the crystallinity of the CS/PEO blended nanofibers. It indicated the formation of a crystalline phase between PEO and CS during the electrospinning process and the excellent polymer compatibility in the blends [Figure 3(d)]. As shown in Figure 3(b), CipHCl had several characteristics peaks at 2θs of 19.04, 24.9, 26.6, and 29.4° due to its regular crystallization.[19,34] Figure 3(c) shows that Moxi also had several characteristics peaks at 2θs of 19.4, 24.4, 27.5, and 29.6°. Blend nanofiber mats loaded with 10 wt % CipHCl and 10 wt % Moxi also had the same peaks at 2θs of 20.16° [Figure 3(f)] and 19.9° [Figure 3(g)], respectively. Figure 3(e) shows the diffractogram of the CS/PEO nanofiber after the GA vapor crosslinking and the characteristic peak was shifted to 19.88°. The results demonstrated that loading the drug did not change the characteristic crystallinity of the CS/PEO blend nanofibrous. The changed peaks corresponding to the crystalline CipHCl and Moxi in CS/PEO nanofibrous containing 10 wt % drug verified that the drug spitted in the polymeric nanofibrous mats was in the amorphous phase.

In Vitro Drug Release of Medicated Nanofiber Mats

The cumulative drugs release from the blend CS/PEO nanofiber mats loaded with different amounts of CipHCl or Moxi are shown in Figure 4. The nanofiber mats loaded with different amounts of drug (5–10 wt %) showed a similar release profile trend. The release profile revealed that the drug-release percentages were 11 and 25.5% for 5 and 10 wt % CipHCl and 9.6 and 14.6% for 5 and 10 wt % Moxi at 3 h, respectively. This indicated that there was no obviously burst release in the initial stage. Then, the release ratio slowed down (72 h) and reached a steady stage along with the incubation time (168 h). Over 168 h of release, 86 and 89% for 5 and 10 wt % CipHCl, respectively, were released and 75 and 77% for 5 and 10 wt % Moxi, respectively, were released. Both CS and CipHCl (Moxi) had a high positive charge density and strong repulsive forces among the polymer chains and drugs; this made CipHCl (Moxi) orient to the surface of the nanofibrous. The high surface area and

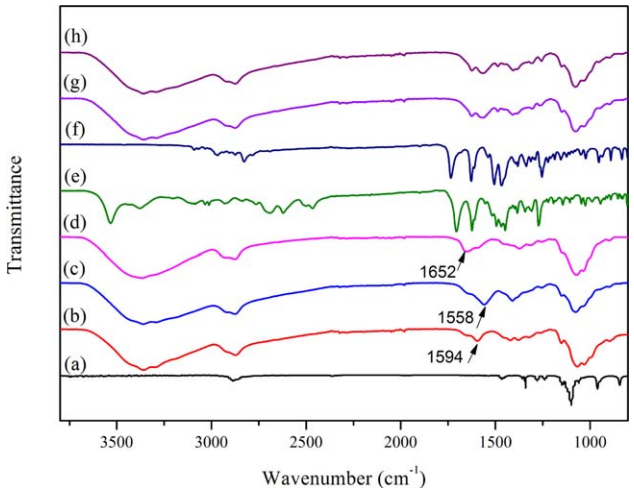

Figure 2. FTIR spectra of the (a) as-spun PEO, (b) CS powder, (c) CS/PEO nanofiber mat, (d) CS/PEO nanofiber mat crosslinked by GA vapor and washed with a glycine solution, (e) CipHCl powder, (f) Moxi powder, (g) CS/PEO nanofiber mat loaded with 10 wt % CipHCl, and (f) CS/PEO nanofiber mat loaded with 10 wt % Moxi. [Color figure can be viewed in the online issue, which is available at wileyonlinelibrary.com.]

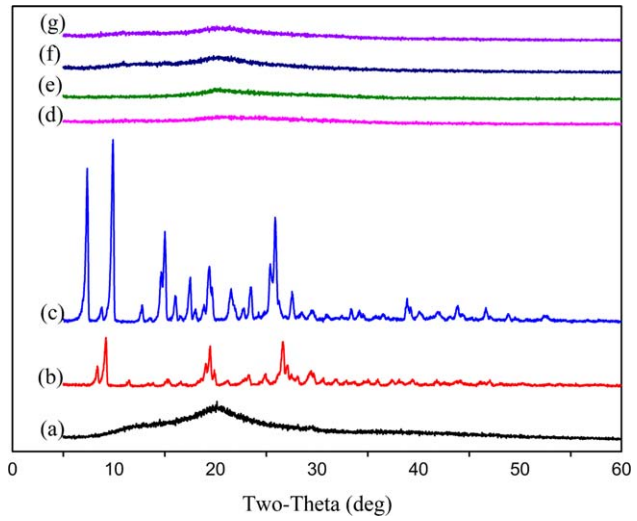

Figure 3. XRD profiles of the (a) CS powder, (b) CipHCl powder, (c) Moxi powder, (d) CS/PEO nanofiber mat, (e) crosslinked CS/PEO nanofiber mat, (f) CS/PEO nanofiber mat loaded with 10 wt % CipHCl, and (g) CS/PEO nanofiber mat loaded with 10 wt % Moxi. [Color figure can be viewed in the online issue, which is available at wileyonlinelibrary.com.]

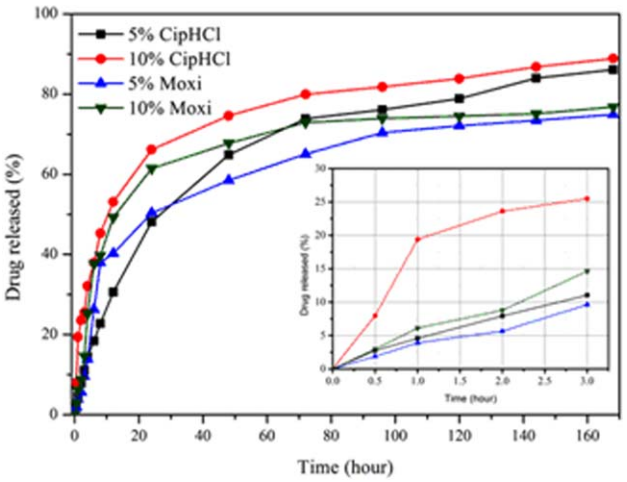

Figure 4. *In vitro* drug-release profiles of the drug–CS/PEO nanofiber mats (pH 7.2–7.4, 37°C). [Color figure can be viewed in the online issue, which is available at wileyonlinelibrary.com.]

porous structure of the nanofibrous membrane enabled the drugs to diffuse into the aqueous medium and to be controlled to release into the medium. Moreover, the CS/PEO nanofiber mats swelled because of the penetration of water through the blend, and this resulted in rapid drug diffusion.

Antibacterial Activity Test

The antibacterial activities of the prepared blend CS/PEO nanofiber mats containing various amount of CipHCl or Moxi were examined against Gram-positive SA and Gram-negative EC by zone of inhibition tests. The results are shown in Figure 5. As shown in Figure 5(a), the inhibition zone of the CS/PEO nanofiber mats without antimicrobial drug enlarged as the CS/PEO spinning solution concentration increased. However, after CipHCl and Moxi were loaded, the inhibition zone became much more clear and fair-sized; this suggested the marked preponderance in the inhibition of the proliferation and growth of bacteria of the drug-loaded samples [Figure 5(b)]. More drug amount was contained in the fiber, and the bigger inhibition

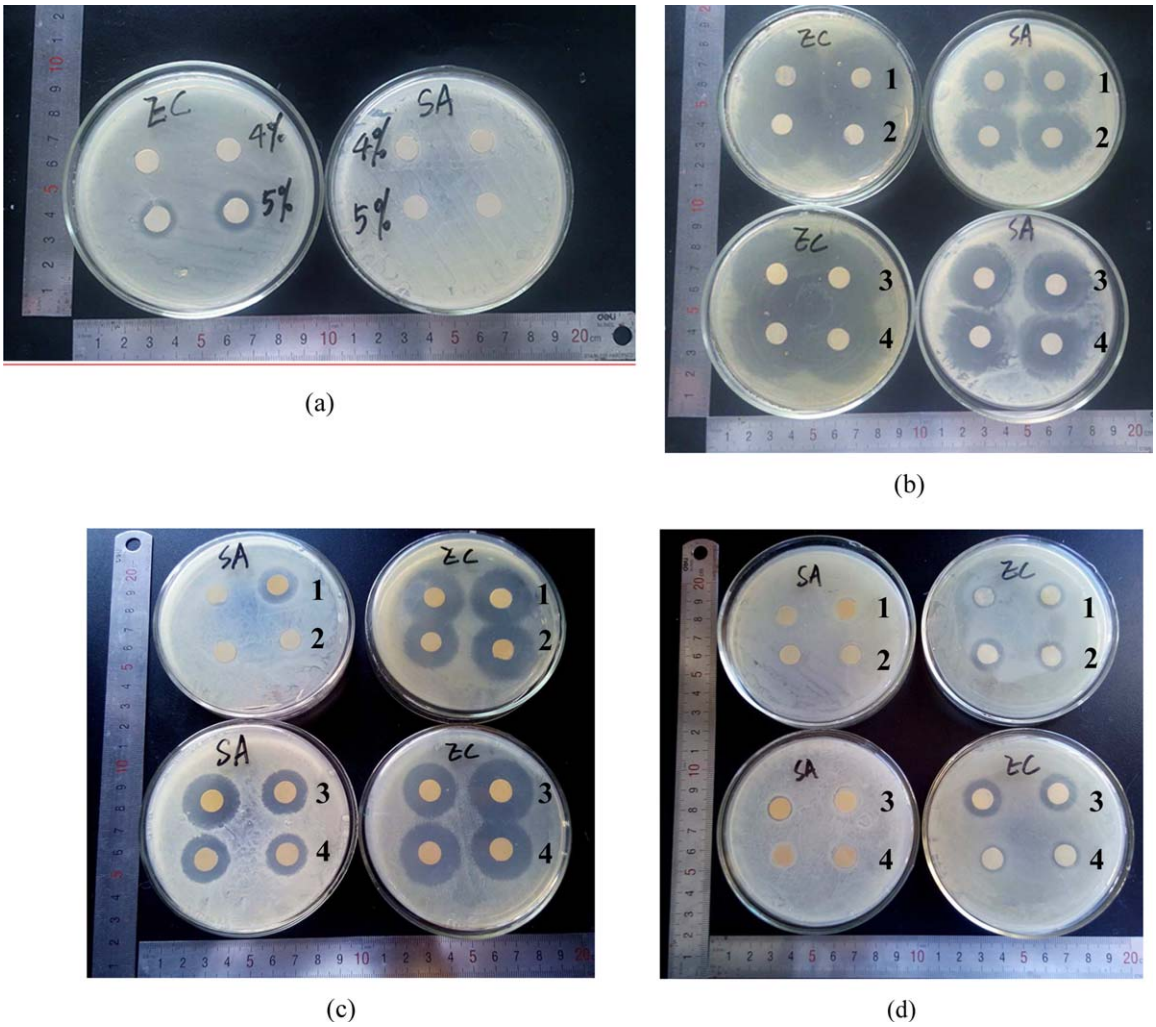

Figure 5. Inhibition zones of (a) 4 and 5% CS/PEO 90/10 nanofiber mats and (b–d) drug–CS/PEO 90/10 nanofiber mats against SA and EC for 24, 48, and 72 h, respectively: (1) 5 wt % CipHCl blended and electrospun with CS/PEO 90/10, (2) 10 wt % CipHCl, (3) 5 wt % Moxi, and (4) 10 wt % Moxi. [Color figure can be viewed in the online issue, which is available at wileyonlinelibrary.com.]

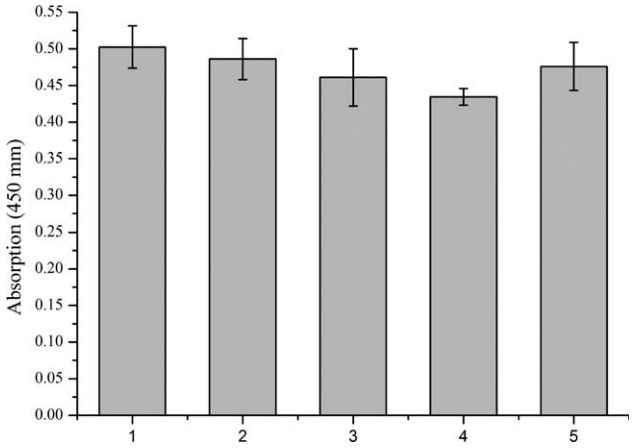

Figure 6. Cytotoxicity assays of the (1) positive control, (2) CS/PEO nanofiber, (3) crosslinked CS/PEO nanofiber mat, (4) 10 wt % CipHCl–CS/PEO nanofiber mat, and (5)10 wt % Moxi–CS/PEO nanofiber mat for positive controls. The data represent the mean values and standard deviations of 12 samples.

zone was formed around the specimen. Moreover, the inhibition zone against EC was generally bigger than that against SA; this demonstrated that the antimicrobial drug was more effective in the inhibition of EC. As shown in Figure 5(c,d), the inhibition zone reduced gradually with time extension because of the decreasing residual drug and the slowing release ratio after 48 and 72 h.

Cytotoxicity Analysis

An ideal wound dressing should be nontoxic to tissues, and this could be evaluated through *in vitro* cytotoxicity assays. The absorbance illustrated the viability of PIECs obtained by ALB assay (Figure 6). No significant differences were observed in the cell viability of PIECs for 24 h in the presence of the CS/PEO nanofiber mats or drug (CipHCl or Moxi)–CS/PEO nanofiber mats in comparison with the positive control, although the average absorbance values were lower than that of the control condition. Absorptions of both the CS/PEO and drug (CipHCl or Moxi)–CS/PEO nanofiber mats before and after crosslinking were above 85% compared with that of the positive control. The results indicate that the obtained drug (CipHCl or Moxi)–CS/PEO nanofiber mats were not obviously toxic to PIECs.

CONCLUSIONS

Continuous uniform nanofiber mats with a high CS/PEO ratio (90/10) loaded with CipHCl or Moxi were successfully electrospun. PEO was miscible with CS to enhance the electrospinnability of CS. SEM images showed that the addition of the drug reduced the electrospun nanofiber diameters because the drugs weakened the interactions between the polymers chains. The antibacterial experiment showed that the nanofiber mats of the drug (CipHCl or Moxi)–CS/PEO had good antimicrobial activity against both the Gram-negative bacteria EC and Gram-positive bacteria SA. The results of the drug-release studies indicate that there was no obvious burst release in the initial stage, and the release ratio slowed down and reached a steady over 168 h; this may be beneficial for prolonged antibacterial activity. Finally, the *in vitro* cytotoxicity assays indicated that the drug (CipHCl or Moxi)–CS/PEO nanofiber mats crosslinked by GA vapor were not obviously toxic to PIECs. The entire results suggest that the obtained drug–CS/PEO nanofiber mats are great potential candidates as wound dressings.

ACKNOWLEDGMENTS

This work was financially supported by the Science & Technology Achievements Transformation and Industrialization Project in Shanghai (contract grant number 14441901600), the Science and Technology Support Program of Jiangsu Province (contract grant number BE2014036), and the Fundamental Research Funds for the Central Universities.

REFERENCES

1. Li, Y.; Chen, F.; Nie, J.; Yang, D. *Carbohydr. Polym.* **2012**, *90*, 1445.
2. Wang, J.; Yao, H. B.; He, D.; Zhang, C. L.; Yu, S. H. *ACS Appl. Mater. Int.* **2012**, *4*, 1963.
3. Fang, X.; Ma, H.; Xiao, S.; Shen, M.; Guo, R.; Cao, X.; Shi, X. *J. Mater. Chem.* **2011**, *21*, 4493.
4. An, J; Zhang, H; Zhang, J; Zhao, Y; Yuan, X. *Colloid Polym. Sci.* **2009**, *287*, 1425.
5. Schiffman, J. D.; Schauer, C. L. *Biomacromolecules* **2007**, *8*, 2665.
6. Dilamian, M.; Montazer, M.; Masoumi, J. *Carbohydr. Polym.* **2013**, *94*, 364.
7. Elsabee, M. Z.; Naguib, H. F.; Morsi, R. E. *Mater. Sci. Eng. C* **2012**, *32*, 1711.
8. Verissimo, D. M.; Leitao, R. F.; Ribeiro, R. A.; Figueiro, S. D.; Sombra, A. S.; Goes, J. C.; Brito, G. A. *Acta Biomater.* **2010**, *6*, 4011.
9. Chen, J.-P; Chang, G.-Y; Chen, J.-K. *Colloid Surf. A* **2008**, *183*, 313.
10. Park, S. A.; Park, K. E.; Kim, W. *Macromol. Res.* **2010**, *18*, 891.
11. Ma, G.; Fang, D.; Liu, Y.; Zhu, X.; Nie, J. *Carbohydr. Polym.* **2012**, *87*, 737.
12. Schneider, A.; Wang, X. Y.; Kaplan, D. L.; Garlick, J. A.; Egles, C. *Acta Biomater.* **2009**, *5*, 2570.
13. Gu, S.-Y.; Wang, Z.-M.; Ren, J.; Zhang, C.-Y. *Mater. Sci. Eng. C* **2009**, *29*, 1822.
14. Zheng, F.; Wang, S.; Wen, S.; Shen, M.; Zhu, M.; Shi, X. *Biomaterials* **2013**, *34*, 1402.
15. Valarezo, E.; Tammaro, L.; González, S.; Malagón, O.; Vittoria, V. *Appl. Clay Sci.* **2013**, *72*, 104.
16. Choi, Y; Nirmala, R; Lee, J. Y; Rahman, M; Hong, S. T; Kim, H. Y. *Ceram. Int.* **2013**, *39*, 4937.
17. Chen, L; Bromberg, L; Lee, J. A; Zhang, H; Schreuder-Gibson, H; Gibson, P; Walker, J; Hammond, P. T; Hatton, T. A; Rutledge, G. C. *Chem. Mater.* **2010**, *22*, 1429.
18. Torres Vargas, E. A.; do Vale Baracho, N. C.; de Brito, J.; de Queiroz, A. A. A. *Acta Biomater.* **2010**, *6*, 1069.

19. Unnithan, A. R.; Barakat, N. A.; Pichiah, P. B.; Gnanasekaran, G.; Nirmala, R.; Cha, Y. S.; Jung, C. H.; El-Newehy, M.; Kim, H. Y. *Carbohydr. Polym.* **2012**, *90*, 1786.
20. Chen, Z; Mo, X; He, C; Wang, H. *Carbohydr. Polym.* **2008**, *72*, 410.
21. Pakravan, M.; Heuzey, M. C.; Ajji, A. *Biomacromolecules* **2012**, *13*, 412.
22. Toskas, G.; Cherif, C.; Hund, R. D.; Laourine, E.; Mahltig, B.; Fahmi, A.; Heinemann, C.; Hanke, T. *Carbohydr. Polym.* **2013**, *94*, 713.
23. Sun, K. *Express Polym. Lett.* **2011**, *5*, 342.
24. Abdelgawad, A. M.; Hudson, S. M.; Rojas, O. J. *Carbohydr. Polym.* **2014**, *100*, 166.
25. McKee, M. G.; Layman, J. M.; Cashion, M. P.; Long, T. E. *Science* **2006**, *311*, 353.
26. Ohkawa, K; Cha, D. I; Kim, H; Nishida, A; Yamamoto, H. *Macromol. Rapid Commun.* **2004**, *25*, 1600.
27. Rakkapao, N.; Vao-Soongnern, V.; Masubuchi, Y.; Watanabe, H. *Polymer* **2011**, *52*, 2618.
28. Kriegel, C.; Kit, K. M.; McClements, D. J.; Weiss, J. *Polymer* **2009**, *50*, 189.
29. Costa-Júnior, E. S.; Barbosa-Stancioli, E. F.; Mansur, A. A. P.; Vasconcelos, W. L.; Mansur, H. S. *Carbohydr. Polym.* **2009**, *76*, 472.
30. Sundaramurthi, D.; Vasanthan, K. S.; Kuppan, P.; Krishnan, U. M.; Sethuraman, S. *Biomed. Mater.* **2012**, *7*, 045005.
31. Zhang, Y.; Huang, X.; Duan, B.; Wu, L.; Li, S.; Yuan, X. *Colloid Polym. Sci.* **2007**, *285*, 855.
32. Kang, Y. O.; Yoon, I. S.; Lee, S. Y.; Kim, D. D.; Lee, S. J.; Park, W. H.; Hudson, S. M. *J. Biomed. Mater. Res. B* **2010**, *92*, 568.
33. Sadri, M; Maleki, A; Agend, F; Hosseini, H. *J. Appl. Polym. Sci.* **2012**, *126*, 2077.
34. Jannesari, M.; Varshosaz, J.; Morshed, M.; Zamani, M. *Int. J. Nanomed.* **2011**, *6*, 993.
35. Dillen, K.; Vandervoort, J.; Van den Mooter, G.; Verheyden, L.; Ludwig, A. *Int. J. Pharm.* **2004**, *275*, 171.
36. Toncheva, A.; Paneva, D.; Maximova, V.; Manolova, N.; Rashkov, I. *Eur. J. Pharm. Sci.* **2012**, *47*, 642.
37. Suzuki, Y. *Biomed. Mater. Res.* **1998**, *42*, 112.
38. Tsou, T.-L. *J. Mater. Sci. Mater. Med.* **2005**, *16*, 95.
39. Pakravan, M.; Heuzey, M.-C.; Ajji, A. *Polymer* **2011**, *52*, 4813.
40. Zamani, M.; Morshed, M.; Varshosaz, J.; Jannesari, M. *Eur. J. Pharm. Biopharm.* **2010**, *75*, 179.
41. Taepaiboon, P.; Rungsardthong, U.; Supaphol, P. *Nanotechnology* **2006**, *17*, 2317.
42. Destaye, A. G.; Lin, C. K.; Lee, C. K. *ACS Appl. Mater. Int.* **2013**, *5*, 4745.
43. Schiffman, J. D.; Schauer, C. L. *Biomacromolecules* **2007**, *8*, 594.